

Neutron diffraction in a model itinerant metal near a quantum critical point

D A Sokolov¹, M C Aronson^{1,2}, R Erwin³, J W Lynn³, M D Lumsden⁴ and S E Nagler⁴

¹ Brookhaven National Laboratory, Upton, NY 11973, USA

² Department of Physics and Astronomy, Stony Brook University, Stony Brook, NY 11794, USA

³ NIST Center for Neutron Research, Gaithersburg, MD 20899, USA

⁴ Neutron Scattering Science Division, Oak Ridge, TN 37831, USA

E-mail: fermiliquid@gmail.com

Abstract. Neutron diffraction measurements on single crystals of $\text{Cr}_{1-x}\text{V}_x$ ($x=0, 0.02, 0.037$) show that the ordering moment and the Neel temperature are continuously suppressed as x approaches 0.037, a proposed Quantum Critical Point (QCP). The wave vector Q of the spin density wave (SDW) becomes more incommensurate as x increases in accordance with the two band model. At $x_C=0.037$ we have found temperature dependent, resolution limited elastic scattering at 4 incommensurate wave vectors $Q=(1\pm\delta_{1,2}, 0, 0)*2\pi/a$, which correspond to 2 SDWs with Neel temperatures of 19 K and 300 K. Our neutron diffraction measurements indicate that the electronic structure of Cr is robust, and that tuning Cr to its QCP results not in the suppression of antiferromagnetism, but instead enables new spin ordering due to novel nesting of the Fermi surface of Cr.

1. Introduction

Cr doped with V has been proposed as an example of an itinerant antiferromagnet, with a second order quantum phase transition [1]. A gradual evolution of the Hall coefficient across the Quantum Critical Point (QCP) was observed, leading to the conclusion that the spin density wave order in $\text{Cr}_{1-x}\text{V}_x$ develops continuously [2]. Spin density order in Cr removes the hot spots of the Fermi surface, which leads to a restructured or nested Fermi surface. In a neutron diffraction experiment, magnetic Bragg scattering is detected at wave vectors equal to nesting wave vectors of the Fermi surface, and its temperature dependence, as well as that of the ordered moment are both measures of the Fermi surface removed by the spin density wave. Although $\text{Cr}_{1-x}\text{V}_x$ was proposed as a model system in which the quantum phase transition of an itinerant antiferromagnet is realized, a detailed neutron scattering study of the spin density wave instability near the proposed quantum critical point in $\text{Cr}_{1-x}\text{V}_x$ is still lacking. Here we report direct measurements of spin density wave ordering by neutron diffraction, carried out on single crystals of $\text{Cr}_{1-x}\text{V}_x$. Our results support the general notion that a quantum phase transition is accompanied by the restructuring of the Fermi surface [3]. The new nesting conditions enabled by the V doping in Cr are responsible for a topological change of the Fermi surface across the QCP.

2. Experimental Details

Single crystals of $\text{Cr}_{1-x}\text{V}_x$ ($x=0.0, 0.02, 0.037$), were grown by the arc zone melting method at the Materials Preparation Center at Ames National Lab. The uniformity of the V doping in the crystals of $\text{Cr}_{1-x}\text{V}_x$ was confirmed by electron microprobe and electron energy loss measurements. Neutron diffraction measurements were carried out on single crystals of $\text{Cr}_{1-x}\text{V}_x$ ($x=0.0, 0.02, 0.037$) using the BT-9 triple-axis spectrometer at the NIST Center for Neutron Research with a fixed final energy $E_F=14.7$ meV. The measurements were performed using a 40'-44'-44'-open collimation configuration. Data were collected near the (1,0,0) and (0,1,0) reciprocal lattice positions in the (001) plane.

3. Results and Discussion

Pure Cr orders antiferromagnetically at 311 K via a spin density wave (SDW) instability. A wavevector Q for the SDW is selected by the nesting condition of the Fermi surface, which consists of electron and hole octahedra. Since the hole Fermi surface is slightly larger than the electron Fermi surface, Q is incommensurate with the lattice. In a neutron diffraction experiment, the incommensurability of Q leads to an observation of 2 magnetic Bragg reflections at $q=2\pi/a(1\pm\delta, 0, 0)$. In the absence of a preferred orientation, Q can lie along any of the 3 cubic axis so in total, 6 satellites can be found near $q=2\pi/a(1, 0, 0)$.

Fig. 1a shows the incommensurate satellites near $q=2\pi/a(1, 0, 0)$ and $q=2\pi/a(0, 1, 0)$, which were probed by transverse and longitudinal scans in pure Cr and $\text{Cr}_{0.98}\text{V}_{0.02}$ below their respective ordering temperatures. Fig. 1b shows a reciprocal plane for $\text{Cr}_{0.963}\text{V}_{0.037}$. At 5 K a longitudinal scan in the $h00$ direction finds two satellites at $q_1=2\pi/a(1\pm\delta_1, 0, 0)$ and two at $q_2=2\pi/a(1\pm\delta_2, 0, 0)$. A transverse scan in the $1k0$ direction finds two satellites at $q_2=2\pi/a(1, 0\pm\delta_2, 0)$ only. The elastic scattering in $\text{Cr}_{0.963}\text{V}_{0.037}$ is resolution limited with respect to the wave vector, corresponding to antiferromagnetic order extending over length scales as large as $\sim 34\text{\AA}$, unexpected for a system very near a QCP.

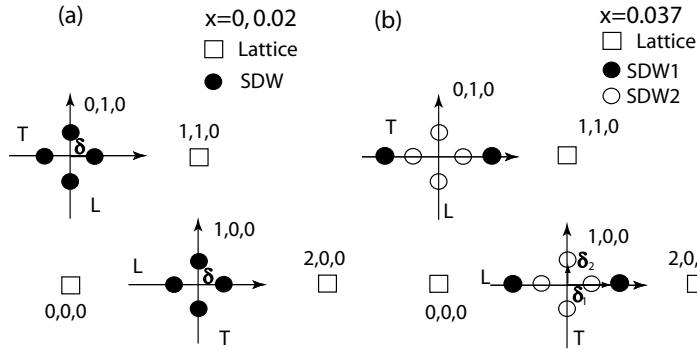


Figure 1. The 001 reciprocal planes of $\text{Cr}_{1-x}\text{V}_x$ probed in our experiments. (a) $x=0, 0.02$, L and T mark the longitudinal and transverse directions of scans. δ is the incommensurability parameter. (b) Same for $x=0.037$.

We refer to scattering at $q_1=2\pi/a(1\pm\delta_1, 0, 0)$ as originating with SDW1, while that at $q_2=2\pi/a(1\pm\delta_2, 0, 0)$ originates with SDW2. Since the scattering at $q_1=2\pi/a(1\pm\delta_1, 0, 0)$ is only observed on longitudinal scans through (1,0,0) or transverse scans through (0,1,0) points in the reciprocal lattice, SDW1 must be transversely polarized with a magnetic moment along (0,0,1). The intensities of the incommensurate satellites at $q_1=2\pi/a(1\pm\delta_1, 0, 0)$ obey the magnetic form factor, confirming that the scattering is magnetic.

In Fig. 2a we plot the temperature dependence of the intensity of the incommensurate satellites in $\text{Cr}_{1-x}\text{V}_x$ ($x=0.0, 0.02, 0.037$). In pure Cr the transition into the SDW state is weakly first order, therefore the incommensurate scattering increases sharply below $T_N=311$ K. Below 122 K, the SDW changes polarisation from transverse to longitudinal, which leads to a loss of intensity at $q=2\pi/a(1\pm\delta, 0, 0)$. In $\text{Cr}_{0.98}\text{V}_{0.02}$ the incommensurate intensity develops gradually

below $T_N=145$ K as an order parameter, indicating that V doping renders the antiferromagnetic transition second order. The intensity increases monotonically on cooling to 5 K suggesting that the polarisation of the SDW in $\text{Cr}_{0.98}\text{V}_{0.02}$ is transverse between 5 K and 145 K.

The incommensurate scattering in $\text{Cr}_{0.963}\text{V}_{0.037}$ is more complex. Scattering at $q_1=2\pi/a(1\pm\delta_1,0,0)$ which corresponds to the most incommensurate satellites, turns on sharply at 19 K, a temperature consistent with the transition temperature obtained from the earlier resistivity measurements [4]. In contrast, the temperature dependence of the incommensurate scattering at $q_2=2\pi/a(1\pm\delta_2,0,0)$ is that of an order parameter with a transition temperature of ~ 300 K. The intensities of scattering at $q=2\pi/a(1\pm\delta_2,0,0)$ and at $q=2\pi/a(0,1\pm\delta_2,0)$ are very similar indicating that our sample is in a multiple- Q state. Below $T=19$ K, SDW1 and SDW2 co-exist.

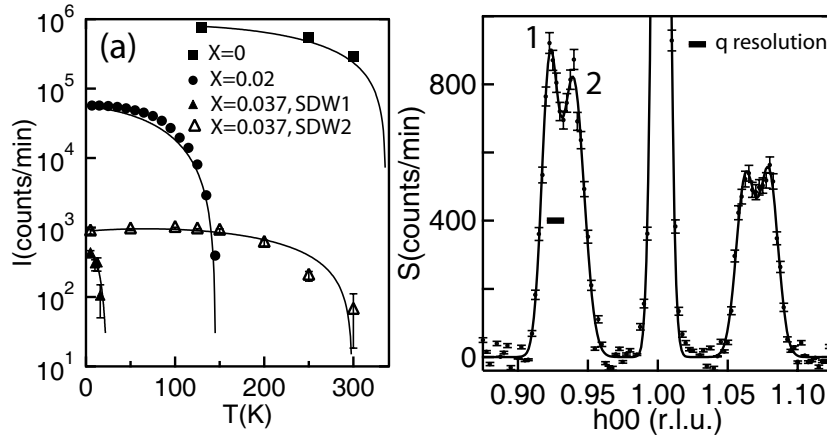


Figure 2. (a) Temperature dependence of the incommensurate scattering in $\text{Cr}_{1-x}\text{V}_x$ $x=0.0, 0.02, 0.037$. Solid lines are order parameter fits. (b) Elastic longitudinal scan through $(1,0,0)$ in $\text{Cr}_{0.963}\text{V}_{0.037}$ collected at 5 K. Bragg peaks 1 and 2 mark SDW1 and SDW2. The solid line is a fit to the data where the fitting function is a sum of 5 gaussian functions plus a linear background. The horizontal solid line is the wave vector resolution of BT-9.

A longitudinal scan through the $(1,0,0)$ point in the reciprocal lattice collected at 5 K in $\text{Cr}_{0.963}\text{V}_{0.037}$ is shown in Fig. 2b. Two separate incommensurate peaks corresponding to SDW1 and SDW2 can be distinguished. The strong commensurate scattering is due to temperature independent $\lambda/2$ contamination from the (200) structural reflection as well as temperature dependent contamination from the $q=2\pi/a(1,0,0\pm\delta)$ satellites, which can be suppressed by tightening of the vertical resolution of the spectrometer.

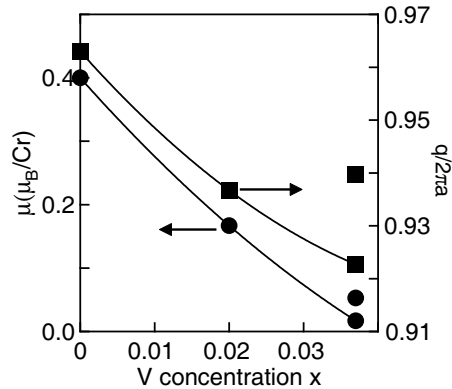


Figure 3. The wavevector of the SDW modulation and the ordering moment in $\text{Cr}_{1-x}\text{V}_x$ as a function of the V concentration measured at 5 K. Solid lines are guides to the eye. Error bars are the size of a marker, or otherwise shown.

To estimate the ordered moment in $\text{Cr}_{0.963}\text{V}_{0.037}$, we have carried out identical neutron diffraction measurements on a single crystal of pure Cr of similar size and shape as the $x=0.037$

doped crystals. The intensities of the (2,0,0) and (1,1,0) structural peaks were very similar in the two crystals, allowing a direct comparison between integrated intensities of the $q=2\pi/a(1,0,0)$ peaks in Cr and $\text{Cr}_{0.963}\text{V}_{0.037}$. The same procedure was followed to estimate the ordered moment in $\text{Cr}_{0.98}\text{V}_{0.02}$. The average moment per Cr in SDW1 in $\text{Cr}_{0.963}\text{V}_{0.037}$ $\langle\mu\rangle=0.017\ \mu_B/\text{Cr}$ at 5 K, a much smaller value than the $\langle\mu\rangle=0.4\ \mu_B/\text{Cr}$ found in pure Cr [5]. In Fig. 3 we show that as the V concentration increases, the ordered moment of the SDW is suppressed and the wavevector becomes more incommensurate. Instead of continuously approaching zero at the QCP, we find that as $x\rightarrow 0.04$ $\text{Cr}_{1-x}\text{V}_x$ develops 2 SDW instabilities at 2 different wavevectors.

It is instructive to compare the neutron diffraction data on V doped Cr with the results of X-ray scattering studies on pure Cr under pressure [6], Fig. 4. Since V has one less electron than Cr, V doping can broadly be considered to expand the hole Fermi surface, driving the ordering wave vector more incommensurate and by reducing the fraction of the total Fermi surface which is nestable, destabilizes antiferromagnetic order and reduces T_N . In contrast, pressure is not thought to significantly change the relative sizes of the electron and hole Fermi surfaces, so the nesting and the Neel temperature are expected to be less strongly affected. Both pressure and doping decrease the lattice parameters, so it is possible to directly compare their respective impacts on the magnetic order at identical lattice spacings. We have compiled values of the Neel temperature in V-doped samples from both our own samples and from the literature, and have compared them to the values derived from high pressure x-ray diffraction measurements in Fig. 4. As the standard electronic model predicts, V doping suppresses T_N much more rapidly than pressure. Whereas the applied pressure monotonically reduces the T_N from 311 K to ~ 90 K at 7 GPa, the V doping reduces the T_N to 19 K at a doping level of only 3.75%. However, the standard electronic model, where nesting of the electron and hole Fermi surfaces stabilizes a single SDW, we find a very different situation near the doping induced quantum critical point. Here, the conventional SDW removes so little of the Fermi surface that the energetics of Cr-V enable a new Fermi surface driven instability, occurring at high temperatures and at a different wave vector, perhaps involving nesting which spans the individual electron or hole surfaces.

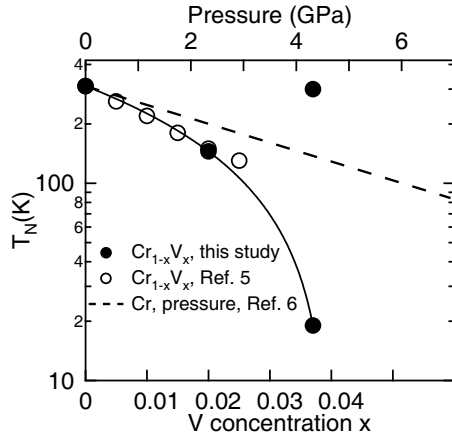


Figure 4. Effects of V doping and external pressure on T_N in Cr. Dashed line represents the data from [6]. Solid lines are guides to the eye. Error bars are the size of a marker, otherwise shown.

In summary, we have shown through neutron diffraction measurements of the spin density wave instabilities that antiferromagnetic order does not vanish near the quantum critical point in Cr which was proposed at the doping level $x\leq 3.75\%$. Instead we find that $\text{Cr}_{0.963}\text{V}_{0.037}$ is a highly ordered system with a new type of antiferromagnetic ordering which persists up to 300 K. This means that the simple Fermi surface nesting model used to describe the SDW instability is no longer appropriate near the quantum critical point and that new theoretical models are needed to explain these novel and co-existing ground states.

3.1. Acknowledgments

D. A. S. and M. C. A. would like to thank A. M. Tsvelik, T. M. Rice, and S. M. Shapiro for useful discussions. Work at BNL and ORNL is supported by the Department of Energy. Work at Stony Brook University is supported by the National Science Foundation.

References

- [1] Yeh A, Soh Y, Brooke J, Aeppli G, Rosenbaum T F and Hayden S M 2002 *Nature* **419** 459
- [2] Lee M, Husmann A, Rosenbaum T F and Aeppli G 2004 *Phys. Rev. Lett.* **92** 187201
- [3] Gegenwart P, Si Q and Steglich F 2008 *Nature Physics* **4** 186
- [4] Sokolov D A, Aronson M C, Strycker G L, Lumsden M D, Nagler S E and Erwin R 2008 *Physica B* **403** 1276
- [5] Koehler W C, Moon R M, Trego A L and Mackintosh A R 1966 *Phys. Rev.* **151** 405.
- [6] Feng Y, Jaramillo R, Srajer G, Lang J C, Islam Z, Somayazulu M S, Shpyrko O G, Pluth J J, Mao H -k, Isaacs E D, Aeppli G and Rosenbaum T F 2007 *Phys. Rev. Lett.* **99** 137201